View metadata, citation and similar papers at core.ac.uk
brought to you by CORE
provided by CERN Document Server

GRAVITATIONAL WAVES FROM COMPACT BODIES

KIP S. THORNE
California Institute of Technology
Pasadena, California USA

1. Introduction

[1] According to general relativity theory, compact concentrations of energy (e.g., neutron stars and black holes) should warp spacetime strongly, and whenever such an energy concentration changes shape, it should create a dynamically changing spacetime warpage that propagates out through the Universe at the speed of light. This propagating warpage is called *gravitational radiation*—a name that arises from general relativity's description of gravity as a consequence of spacetime warpage.

There are a number of efforts, worldwide, to detect gravitational radiation. These efforts are driven in part by the desire to "see gravitational waves in the flesh," but more importantly by the goal of using the waves as a probe of the Universe and of the nature of gravity. They should be a powerful probe, since they carry very detailed information about gravity and their sources.

In this lecture I shall describe the prospects to study gravitational waves from astronomical systems that exist in our Universe today. Such systems are expected to radiate in the "high-frequency" (1—10^4Hz) and "low-frequency" (10^{-4}—1Hz) gravitational-wave bands. By contrast, gravitational waves from the early universe (which I shall not discuss here) should populate a far wider band of frequencies, $\sim 10^{-18}$Hz—10^{+8}Hz.

The high-frequency band is the domain of Earth-based gravitational-wave detectors: resonant-mass antennas, and most especially laser interferometers. A number of interesting compact sources fall in this band: the stellar collapse to a neutron star or black hole in our Galaxy and distant

[1]This paper will be published in *Proceedings of IAU Symposium 165, Compact Stars in Binaries,* edited by J. van Paradijs, E. van den Heuvel, and E. Kuulkers (Kluwer Academic Publishers).

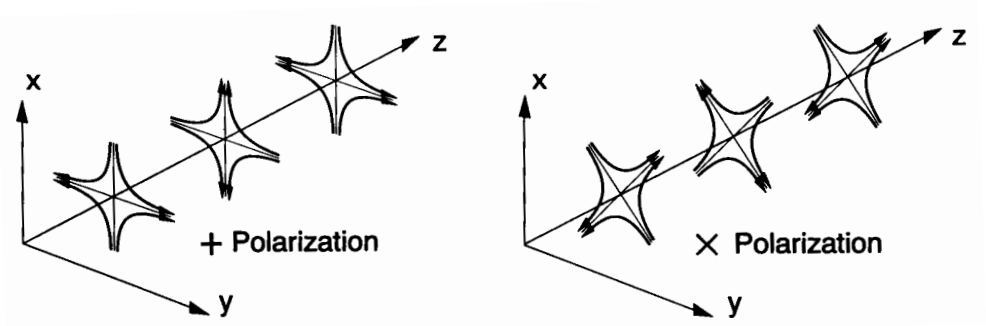

Figure 1. The lines of force associated with the two polarizations of a gravitational wave. (From Ref. [1].)

galaxies, which triggers supernovae; the rotation and vibration of neutron stars in our Galaxy; and the coalescence of neutron-star and stellar-mass black-hole binaries ($M \lesssim 1000 M_\odot$) in distant galaxies.

The low-frequency band is the domain of detectors flown in space (in Earth orbit or in interplanetary orbit). The most important of these are the Doppler tracking of spacecraft via microwave signals sent from Earth to the spacecraft and there transponded back to Earth (a technique that NASA has pursued since the early 1970's), and optical tracking of spacecraft by each other (laser interferometry in space, a technique now under development for possible flight in $\sim$ 2014). The low-frequency band should be populated by waves from short-period binary stars in our own Galaxy (main-sequence binaries, cataclysmic variables, white-dwarf binaries, neutron-star binaries, ...); by waves from white dwarfs, neutron stars, and small black holes spiraling into massive black holes ($M \sim 3 \times 10^5$ to $3 \times 10^7 M_\odot$) in distant galaxies; and by waves from the inspiral and coalescence of massive black-hole binaries ($M \sim 100$ to $10^8 M_\odot$) in distant galaxies.

The body of this lecture consists of four principal sections. Section 2 describes a network of high-frequency, ground-based laser interferometers that is currently under construction, and then Sec. 3 describes the high-frequency sources the network will search for, and the information that we hope to glean from their waves. Section 4 describes a system of low-frequency, space-based interferometers planned for launch in $\sim$ 2014, and Sec. 5 describes the low-frequency sources they will search for and the information carried by their waves.

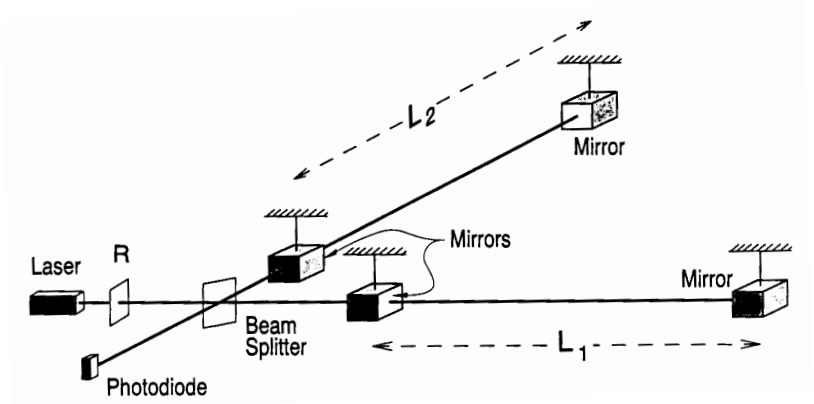

Figure 2. Schematic diagram of a laser interferometer gravitational wave detector. (From Ref. [1].)

2. Ground-Based Laser Interferometers

2.1. WAVE POLARIZATIONS, WAVEFORMS, AND HOW AN INTERFEROMETER WORKS

According to general relativity theory, a gravitational wave has two linear polarizations, conventionally called + (plus) and × (cross). Associated with each polarization there is a gravitational-wave field, h_+ or $h_\times$, which oscillates in time and propagates with the speed of light. Each wave field produces tidal forces (gravitational stretching and squeezing forces) on any object or detector through which it passes. If the object is small compared to the waves' wavelength (as is the case for ground-based interferometers and resonant mass antennas), then relative to the object's center, the forces have the quadrupolar patterns shown in Figure 1. The names "plus" and "cross" are derived from the orientations of the axes that characterize the force patterns [2].

A laser interferometer gravitational wave detector ("interferometer" for short) consists of four masses that hang from vibration-isolated supports as shown in Figure 2, and the indicated optical system for monitoring the separations between the masses [2, 1]. Two masses are near each other, at the corner of an "L", and one mass is at the end of each of the L's long arms. The arm lengths are nearly equal, $L_1 \simeq L_2 = L$. When a gravitational wave, with frequencies high compared to the masses' $\sim$ 1 Hz pendulum frequency, passes through the detector, it pushes the masses back and forth relative to each other as though they were free from their suspension wires, thereby changing the arm-length difference, $\Delta L \equiv L_1 - L_2$. That change is monitored by laser interferometry in such a way that the output of the photodiode (the interferometer's output) is directly proportional to $\Delta L(t)$.

If the gravitational waves are coming from overhead or underfoot and the axes of the + polarization coincide with the arms' directions, then it is the waves' + polarization that drives the masses, and $\Delta L(t)/L = h_+(t)$. More generally, the interferometer's output is a linear combination of the two wave fields:

$$\frac{\Delta L(t)}{L} = F_+ h_+(t) + F_\times h_\times(t) \equiv h(t) \; . \tag{1}$$

The coefficients F_+ and $F_\times$ are of order unity and depend in a quadrupolar manner on the direction to the source and the orientation of the detector [2]. The combination $h(t)$ of the two waveforms is called the *gravitational-wave strain* that acts on the detector; and the time evolutions of $h(t)$, $h_+(t)$, and $h_\times(t)$ are sometimes called *waveforms*.

2.2. WAVE STRENGTHS AND INTERFEROMETER ARM LENGTHS

The strengths of the waves from a gravitational-wave source can be estimated using the "Newtonian/quadrupole" approximation to the Einstein field equations. This approximation says that $h \simeq (G/c^4)\ddot{Q}/r$, where $\ddot{Q}$ is the second time derivative of the source's quadrupole moment, r is the distance of the source from Earth, and G and c are Newton's gravitation constant and the speed of light. The strongest sources will be highly nonspherical and thus will have $Q \simeq ML^2$, where M is their mass and L their size, and correspondingly will have $\ddot{Q} \simeq 2Mv^2 \simeq 4E^{\rm ns}_{\rm kin}$, where v is their internal velocity and $E^{\rm ns}_{\rm kin}$ is the nonspherical part of their internal kinetic energy. This provides us with the estimate

$$h \sim \frac{1}{c^2}\frac{4G(E^{\rm ns}_{\rm kin}/c^2)}{r} \; ; \tag{2}$$

i.e., h is about 4 times the gravitational potential produced at Earth by the mass-equivalent of the source's nonspherical, internal kinetic energy—made dimensionless by dividing by c^2. Thus, in order to radiate strongly, the source must have a very large, nonspherical, internal kinetic energy.

The best known way to achieve a huge internal kinetic energy is via gravity; and by energy conservation (or the virial theorem), any gravitationally-induced kinetic energy must be of order the source's gravitational potential energy. A huge potential energy, in turn, requires that the source be very compact, not much larger than its own gravitational radius. Thus, the strongest gravity-wave sources must be highly compact, dynamical concentrations of large amounts of mass (e.g., colliding and coalescing black holes and neutron stars).

Such sources cannot remain highly dynamical for long; their motions will be stopped by energy loss to gravitational waves and/or the formation

of an all-encompassing black hole. Thus, the strongest sources should be transient. Moreover, they should be very rare — so rare that to see a reasonable event rate will require reaching out through a substantial fraction of the Universe. Thus, just as the strongest radio waves arriving at Earth tend to be extragalactic, so also the strongest gravitational waves are likely to be extragalactic.

For highly compact, dynamical objects that radiate in the high-frequency band, e.g. colliding and coalescing neutron stars and stellar-mass black holes, the internal, nonspherical kinetic energy $E^{\rm ns}_{\rm kin}/c^2$ is of order the mass of the Sun; and, correspondingly, Eq. (2) gives $h \sim 10^{-22}$ for such sources at the Hubble distance, $h \sim 10^{-21}$ at 200 Mpc (a best-guess distance for several neutron-star coalescences per year; Sec. 3.1.2), and $h \sim 10^{-20}$ at the Virgo cluster (15 Mpc). These numbers set the scale of sensitivities that ground-based interferometers seek to achieve: $h \lesssim 10^{-21}$ to 10^{-22}.

When one examines the technology of laser interferometry, one sees good prospects to achieve measurement accuracies $\Delta L \sim 10^{-16}$ cm (1/1000 the diameter of the nucleus of an atom). With such an accuracy, an interferometer must have an arm length $L = \Delta L/h \sim 1$ to 10 km, in order to achieve the desired wave sensitivities, 10^{-21} to 10^{-22}. This sets the scale of the interferometers that are now under construction.

2.3. LIGO, VIRGO, AND THE INTERNATIONAL INTERFEROMETRIC NETWORK

Interferometers are plagued by non-Gaussian noise, e.g. due to sudden strain releases in the wires that suspend the masses. This noise prevents a single interferometer, by itself, from detecting with confidence short-duration gravitational-wave bursts (though it might be possible for a single interferometer to search for the periodic waves from known pulsars). The non-Gaussian noise can be removed by cross correlating two, or preferably three or more, interferometers that are networked together at widely separated sites.

The technology and techniques for such interferometers have been under development for nearly 25 years, and plans for km-scale interferometers have been developed over the past 13 years. An international network consisting of three km-scale interferometers, at three widely separated sites, is now in the early stages of construction. It includes two sites of the American LIGO Project ("Laser Interferometer Gravitational Wave Observatory") [1], and one site of the French/Italian VIRGO Project (named after the Virgo cluster of galaxies) [3].

LIGO will consist of two vacuum facilities with 4-kilometer-long arms, one in Hanford, Washington (in the northwestern United States) and the other in Livingston, Louisiana (in the southeastern United States). These

facilities are designed to house many successive generations of interferometers without the necessity of any major facilities upgrade; and after a planned future expansion, they will be able to house several interferometers at once, each with a different optical configuration optimized for a different type of wave (e.g., broad-band burst, or narrow-band periodic wave, or stochastic wave). The LIGO facilities and their first interferometers are being constructed by a team of about 80 physicists and engineers at Caltech and MIT, led by Barry Barish (the PI) and Gary Sanders (the Project Manager). Substantial contributions are also being made by scientists at other institutions.

The VIRGO Project is building one vacuum facility in Pisa, Italy, with 3-kilometer-long arms. This facility and its first interferometers are a collaboration of more than a hundred physicists and engineers at the INFN (Frascati, Napoli, Perugia, Pisa), LAL (Orsay), LAPP (Annecy), LOA (Palaiseau), IPN (Lyon), ESPCI (Paris), and the University of Illinois (Urbana), under the leadership of Alain Brillet and Adalberto Giazotto.

Both LIGO and VIRGO are scheduled for completion in the late 1990s, and their first gravitational-wave searches are likely to be performed in 2000 or 2001.

LIGO alone, with its two sites which have parallel arms, will be able to detect an incoming gravitational wave, measure one of its two waveforms, and (from the time delay between the two sites) locate its source to within a $\sim 1^{\rm o}$ wide annulus on the sky. LIGO and VIRGO together, operating as a *coordinated international network*, will be able to locate the source (via time delays plus the interferometers' beam patterns) to within a 2-dimensional error box with size between several tens of arcminutes and several degrees, depending on the source direction and on the amount of high-frequency structure in the waveforms. They will also be able to monitor both waveforms $h_+(t)$ and $h_\times(t)$ (except for frequency components above about 1kHz and below about 10 Hz, where the interferometers' noise becomes severe).

The accuracies of the direction measurements and the ability to monitor more than one waveform will be severely compromised when the source lies anywhere near the plane formed by the three LIGO/VIRGO interferometer locations. To get good all-sky coverage will require a fourth interferometer at a site far out of that plane; Japan and Australia would be excellent locations, and research groups there are carrying out research and development on interferometric detectors, aimed at such a possibility. A 300-meter prototype interferometer called TAMA is under construction in Tokyo, and a 400-meter prototype called AIGO400 has been proposed for construction north of Perth.

Two other groups are major players in this field, one in Britain led by

James Hough, the other in Germany, led by Karsten Danzmann. These groups each have two decades of experience with prototype interferometers (comparable experience to the LIGO team and far more than anyone else) and great expertise. Frustrated by inadequate financing for a kilometer-scale interferometer, they are constructing, instead, a 600 meter system called GEO600 near Hannover, Germany. Their goal is to develop, from the outset, an interferometer with the sort of advanced design that LIGO and VIRGO will attempt only as a "second-generation" instrument, and thereby achieve sufficient sensitivity to be full partners in the international network's first gravitational-wave searches; they then would offer a variant of their interferometer as a candidate for second-generation operation in the much longer arms of LIGO and/or VIRGO. It is a seemingly audacious plan, but with their extensive experience and expertise, the British/German collaboration might pull it off successfully.

3. High-Frequency Gravitational-Wave Sources

3.1. COALESCING COMPACT BINARIES

The best understood of all gravitational-wave sources are coalescing, compact binaries composed of neutron stars (NS) and black holes (BH). These NS/NS, NS/BH, and BH/BH binaries may well become the "bread and butter" of the LIGO/VIRGO diet.

The Hulse-Taylor [4, 5] binary pulsar, PSR 1913+16, is an example of a NS/NS binary whose waves could be measured by LIGO/VIRGO, if we were to wait long enough. At present PSR1913+16 has an orbital frequency of about 1/(8 hours) and emits its waves predominantly at twice this frequency, roughly 10^{-4} Hz, which is in the low-frequency band—far too low to be detected by LIGO/VIRGO. However, as a result of their loss of orbital energy to gravitational waves, the PSR1913+16 NS's are gradually spiraling inward. If we wait roughly 10^8 years, this inspiral will bring the waves into the LIGO/VIRGO high-frequency band. As the NS's continue their inspiral, the waves will then sweep upward in frequency, over a time of about 15 minutes, from 10 Hz to $\sim 10^3$ Hz, at which point the NS's will collide and coalesce. It is this last 15 minutes of inspiral, with $\sim 16,000$ cycles of waveform oscillation, and the final coalescence, that LIGO/VIRGO seeks to monitor.

3.1.1. *Wave Strengths Compared to LIGO Sensitivities*

Figure 3 compares the projected sensitivities of interferometers in LIGO [1] with the wave strengths from the last few minutes of inspiral of BH/BH, NS/BH, and NS/NS binaries at various distances from Earth. The two solid curves at the bottoms of the stippled regions (labeled $h_{\rm rms}$) are the rms noise

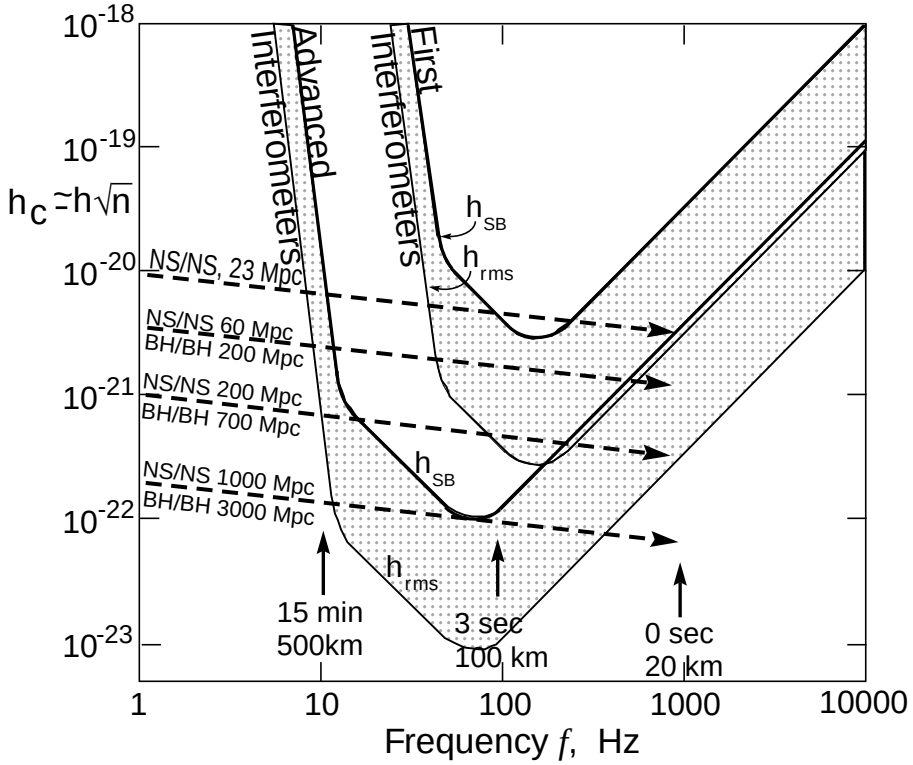

Figure 3. LIGO's projected broad-band noise $h_{\rm rms}$ and sensitivity to bursts $h_{\rm SB}$ [1] compared with the strengths of the waves from the last few minutes of inspiral of compact binaries. The signal to noise ratios are $\sqrt{2}$ higher than in Ref. [1] because of a factor 2 error in Eq. (29) of Ref. [2].

levels for broad-band waves that have optimal direction and polarization. The tops of the stippled regions (labeled $h_{\rm SB}$ for "sensitivity to bursts") are the sensitivities for highly confident detection of randomly polarized, broad-band waves from random directions (i.e., the sensitivities for high confidence that any such observed signal is not a false alarm due to Gaussian noise). The upper stippled region and its bounding curves are the expected performances of the first interferometers in LIGO; the lower stippled region and curves are performances of more advanced LIGO interferometers.

As the NS's and/or BH's spiral inward, their waves sweep upward in frequency (left to right in the diagram). The dashed lines show their "characteristic" signal strength h_c (approximately the amplitude h of the waves' oscillations multiplied by the square root of the number of cycles spent near a given frequency, $\sqrt{n}$); the signal-to-noise ratio is this h_c divided by the detector's $\sqrt{5}h_{\rm rms}$, $S/N = h_c/(\sqrt{5}h_{\rm rms})$, where the $\sqrt{5}$ converts $h_{\rm rms}$ from "optimal direction and polarization" to "random direction and polariza-

tion") [1, 2]. The arrows along the NS/NS inspiral track indicate the time until final coalescence and the separation between the NS centers of mass. Each NS is assumed to have a mass of 1.4 suns and a radius ~ 10 km; each BH, 10 suns and ~ 20 km.

Notice that the signal strengths in Fig. 3 are in good accord with rough estimates based on Eq. (2); at the endpoint (right end) of each inspiral, the number of cycles n spent near that frequency is of order unity, so the quantity plotted, $h_c \simeq h\sqrt{n}$, is about equal to h—and at distance 200 Mpc is about 10^{-21}, as Eq. (2) predicts.

3.1.2. *Coalescence Rates*

Such final coalescences are few and far between in our own galaxy: about one every 100,000 years, according to 1991 estimates by Phinney [6] and by Narayan, Piran, and Shemi [7], based on the statistics of binary pulsar searches in our galaxy which found three that will coalesce in less than 10^{10} years. Extrapolating out through the universe on the basis of the density of production of blue light (the color produced predominantly by massive stars), Phinney [6] and Narayan et. al. [7] infer that to see several NS/NS coalescences per year, LIGO/VIRGO will have to look out to a distance of about 200 Mpc (give or take a factor ~ 2); cf. the "NS/NS inspiral, 200 Mpc" line in Fig. 3. Since these estimates were made, the binary pulsar searches have been extended through a significantly larger volume of the galaxy than before, and no new ones with coalescence times $\lesssim 10^{10}$ years have been found; as a result, the binary-pulsar-search-based best estimate of the coalescence rate should be revised downward [8], perhaps to as little as one every million years in our galaxy, corresponding to a distance 400 Mpc for several per year [8].

A rate of one every million years in our galaxy is ~ 1000 times smaller than the birth rate of the NS/NS binaries' progenitors: massive, compact, main-sequence binaries [6, 7]. Therefore, either 99.9 per cent of progenitors fail to make it to the NS/NS state (e.g., because of binary disruption during a supernova or forming TŻO's), or else they do make it, but they wind up as a class of NS/NS binaries that has not yet been discovered in any of the pulsar searches. Several experts on binary evolution have argued for the latter [9, 10, 11, 12]: most NS/NS binaries, they suggest, may form with such short orbital periods that their lifetimes to coalescence are significantly shorter than normal pulsar lifetimes ($\sim 10^7$ years); and with such short lifetimes, they have been missed in pulsar searches. By modeling the evolution of the galaxy's binary star population, the binary experts arrive at best estimates as high as 3×10^{-4} coalescences per year in our galaxy, corresponding to several per year out to 60 Mpc distance [9]. Phinney [6] describes other plausible populations of NS/NS binaries that could increase

the event rate, and he argues for "ultraconservative" lower and upper limits of 23 Mpc and 1000Mpc for how far one must look to see several coalescence per year.

By comparing these rate estimates with the signal strengths in Fig. 3, we see that (i) the first interferometers in LIGO/VIRGO have a moderate but not high probability of seeing NS/NS coalescences; (ii) advanced interferometers are almost certain of seeing them (the requirement that this be so was one factor that forced the LIGO/VIRGO arm lengths to be so long, several kilometers); and (iii) they are most likely to be discovered roughly half-way between the first and advanced interferometers—which means by an improved variant of the first interferometers several years after LIGO operations begin.

We have no good observational handle on the coalescence rate of NS/BH or BH/BH binaries. However, theory suggests that their progenitors might not disrupt during the stellar collapses that produce the NS's and BH's, so their coalescence rate could be about the same as the birth rate for their progenitors: $\sim 1/100,000$ years in our galaxy. This suggests that within 200 Mpc distance there might be several NS/BH or BH/BH coalescences per year. [6, 7, 9, 12]. This estimate should be regarded as a plausible upper limit on the event rate and lower limit on the distance to look [6, 7].

If this estimate is correct, then NS/BH and BH/BH binaries will be seen before NS/NS, and might be seen by the first LIGO/VIRGO interferometers or soon thereafter; cf. Fig. 3. However, this estimate is far less certain than the (rather uncertain) NS/NS estimates!

Once coalescence waves have been discovered, each further improvement of sensitivity by a factor 2 will increase the event rate by $2^3 \simeq 10$. Assuming a rate of several NS/NS per year at 200 Mpc, the advanced interferometers of Fig. 3 should see ~ 100 per year.

3.1.3. *Inspiral Waveforms and the Information They Can Bring*

Neutron stars and black holes have such intense self gravity that it is exceedingly difficult to deform them. Correspondingly, as they spiral inward in a compact binary, they do not gravitationally deform each other significantly until several orbits before their final coalescence [13, 14]. This means that the inspiral waveforms are determined to high accuracy by only a few, clean parameters: the masses and spin angular momenta of the bodies, and the initial orbital elements (i.e. the elements when the waves enter the LIGO/VIRGO band).

Though tidal deformations are negligible during inspiral, relativistic effects can be very important. If, for the moment, we ignore the relativistic effects—i.e., if we approximate gravity as Newtonian and the wave gener-

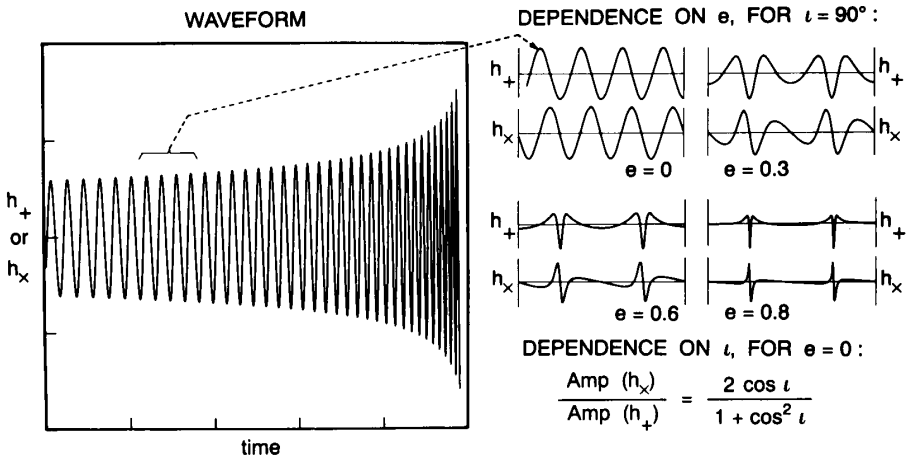

Figure 4. Waveforms from the inspiral of a compact binary, computed using Newtonian gravity for the orbital evolution and the quadrupole moment approximation for the wave generation. (From Ref. [1].)

ation as due to the binary's oscillating quadrupole moment [2], then the shapes of the inspiral waveforms $h_+(t)$ and $h_\times(t)$ are as shown in Fig. 4.

The left-hand graph in Fig. 4 shows the waveform increasing in amplitude and sweeping upward in frequency (i.e., undergoing a "chirp") as the binary's bodies spiral closer and closer together. The ratio of the amplitudes of the two polarizations is determined by the inclination ι of the orbit to our line of sight (lower right in Fig. 4). The shapes of the individual waves, i.e. the waves' harmonic content, are determined by the orbital eccentricity (upper right). (Binaries produced by normal stellar evolution should be highly circular due to past radiation reaction forces, but compact binaries that form by capture events, in dense star clusters that might reside in galactic nuclei [15], could be quite eccentric.) If, for simplicity, the orbit is circular, then the rate at which the frequency sweeps or "chirps", df/dt [or equivalently the number of cycles spent near a given frequency, $n = f^2(df/dt)^{-1}$] is determined solely, in the Newtonian/quadrupole approximation, by the binary's so-called *chirp mass*, $M_c \equiv (M_1 M_2)^{3/5}/(M_1 + M_2)^{1/5}$ (where M_1 and M_2 are the two bodies' masses). The amplitudes of the two waveforms are determined by the chirp mass, the distance to the source, and the orbital inclination. Thus (in the Newtonian/quadrupole approximation), by measuring the two amplitudes, the frequency sweep, and the harmonic content of the inspiral waves, one can determine as direct, resulting observables, the source's distance, chirp mass, inclination, and eccentricity [16, 17].

As in binary pulsar observations [5], so also here, relativistic effects add further information: they influence the rate of frequency sweep and produce waveform modulations in ways that depend on the binary's di-

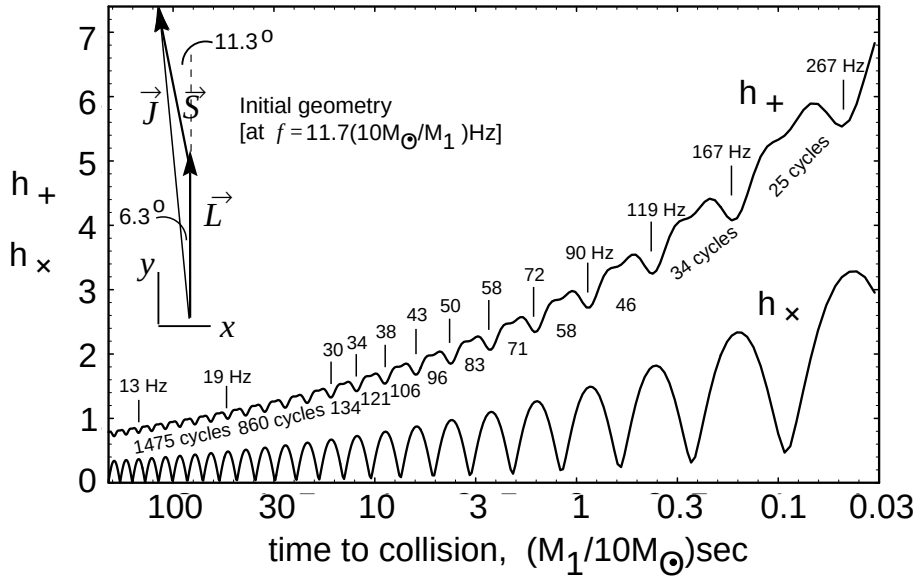

Figure 5. Modulational envelope for the waveform from a $1M_\odot$ nonspinning NS spiraling into a $10M_\odot$, rapidly spinning Kerr black hole (spin parameter $a = 1$). The orbital angular momentum $\mathbf{L}$ is inclined by $\alpha = 11.3$ degrees to the hole's spin angular momentum $\mathbf{S}$, and the two precess around $\mathbf{J} = \mathbf{L} + \mathbf{S}$, whose direction remains fixed in space as $L = |\mathbf{L}|$ shrinks and $S = |\mathbf{S}| = M_{\rm BH}a$ remains constant. The precession modulates the waves by an amount that depends on (i) the direction to Earth (here along the initial $\mathbf{L}\times\mathbf{S}$, i.e. out of the paper) and (ii) the orientation of the detector's arms (here parallel to the figure's initial $\mathbf{L}$ and to $\mathbf{L}\times$(direction to Earth) for h_+, and rotated 45 degrees for $h_\times$). The figure shows the waveforms' modulational envelopes (in arbitrary units, the same for h_+ and $h_\times$), parametrized by the wave frequency f and the number of cycles of *oscillation* between the indicated f's. The total number of *precessions* from f to coalescence is $N_{\rm prec} \simeq (5/64\pi)(Ma/\mu)(\pi Mf)^{-2/3} \simeq 20(f/10{\rm Hz})^{-2/3}$. (From [18, 19].)

mensionless ratio $\eta = \mu/M$ of reduced mass $\mu = M_1M_2/(M_1 + M_2)$ to total mass $M = M_1 + M_2$ [20] and on the spins of the binary's two bodies [21]; These relativistic effects are reviewed and discussed at length in Refs. [18, 22]. Two deserve special mention: (i) As the waves emerge from the binary, some of them get backscattered one or more times off the binary's spacetime curvature, producing wave *tails*. These tails act back on the binary, modifying its inspiral rate in a measurable way. (ii) If the orbital plane is inclined to one or both of the binary's spins, then the spins drag inertial frames in the binary's vicinity (the "Lense-Thirring effect"), this frame dragging causes the orbit to precess, and the precession modulates the waveforms [18, 19, 23]. Figure 5 shows the resulting modulation for a $1M_\odot$ NS spiraling into a rapidly spinning, $10M_\odot$ BH.

Remarkably, the relativistic corrections to the frequency sweep will be measurable with very high accuracy, even though they are typically $\lesssim 10$

per cent of the Newtonian contribution, and even though the typical signal to noise ratio will be only ~ 9 even after optimal signal processing. The reason is as follows [24, 25, 18]:

The frequency sweep will be monitored by the method of "matched filters"; in other words, the incoming, noisy signal will be cross correlated with theoretical templates. If the signal and the templates gradually get out of phase with each other by more than $\sim 1/10$ cycle as the waves sweep through the LIGO/VIRGO band, their cross correlation will be significantly reduced. Since the total number of cycles spent in the LIGO/VIRGO band will be $\sim 16,000$ for a NS/NS binary, ~ 3500 for NS/BH, and ~ 600 for BH/BH, this means that LIGO/VIRGO should be able to measure the frequency sweep to a fractional precision $\lesssim 10^{-4}$, compared to which the relativistic effects are very large. (This is essentially the same method as Joseph Taylor and colleagues use for high-accuracy radio-wave measurements of relativistic effects in binary pulsars [5].)

Preliminary analyses, using the theory of optimal signal processing, predict the following typical accuracies for LIGO/VIRGO measurements based solely on the frequency sweep (i.e., ignoring modulational information) [26, 24, 25, 27, 18]: (i) The chirp mass M_c will typically be measured, from the Newtonian part of the frequency sweep, to $\sim 0.04\%$ for a NS/NS binary and $\sim 0.3\%$ for a system containing at least one BH. (ii) *If* we are confident (e.g., on a statistical basis from measurements of many previous binaries) that the spins are a few percent or less of the maximum physically allowed, then the reduced mass μ will be measured to $\sim 1\%$ for NS/NS and NS/BH binaries, and $\sim 3\%$ for BH/BH binaries. (Here and below NS means a $\sim 1.4M_\odot$ neutron star and BH means a $\sim 10M_\odot$ black hole.) (iii) Because the frequency dependences of the (relativistic) μ effects and spin effects are not sufficiently different to give a clean separation between μ and the spins, if we have no prior knowledge of the spins, then the spin/μ correlation will worsen the typical accuracy of μ by a large factor, to $\sim 30\%$ for NS/NS, $\sim 50\%$ for NS/BH, and a factor ~ 2 for BH/BH [26, 24]. These worsened accuracies might be improved somewhat by waveform modulations caused by the spin-induced precession of the orbit [19, 23], and even without modulational information, a certain combination of μ and the spins will be determined to a few per cent. Much additional theoretical work is needed to firm up the measurement accuracies.

To take full advantage of all the information in the inspiral waveforms will require theoretical templates that are accurate, for given masses and spins, to a fraction of a cycle during the entire sweep through the LIGO/VIRGO band. Such templates are being computed by an international consortium of relativity theorists (Blanchet and Damour in France, Iyer in India, Will and Wiseman in the U.S., and others) [22, 28], using

post-Newtonian expansions of the Einstein field equations. This enterprise is rather like computing the Lamb shift to high order in powers of the fine structure constant, for comparison with experiment. The terms of leading order in the mass ratio $\eta = \mu/M$ are being checked by a Japanese-American consortium (Poisson, Nakamura, Sasaki, Tagoshi, Tanaka) using the Teukolsky formalism for weak perturbations of black holes [29, 30]. These small-η calculations have been carried to very high post-Newtonian order for circular orbits and no spins [31, 32], and from those results Cutler and Flanagan [33] have estimated the order to which the full, finite-η computations must be carried in order that systematic errors in the theoretical templates will not significantly impact the information extracted from the LIGO/VIRGO observational data. The answer appears daunting: radiation-reaction effects must be computed to three full post-Newtonian orders [six orders in v/c =(orbital velocity)/(speed of light)] beyond the leading-order radiation reaction, which itself is 5 orders in v/c beyond the Newtonian theory of gravity.

It is only about ten years since controversies over the leading-order radiation reaction [34] were resolved by a combination of theoretical techniques and binary pulsar observations. Nobody dreamed then that LIGO/VIRGO observations will require pushing post-Newtonian computations onward from $O[(v/c)^5]$ to $O[(v/c)^{11}]$. This requirement epitomizes a major change in the field of relativity research: At last, 80 years after Einstein formulated general relativity, experiment has become a major driver for theoretical analyses.

Remarkably, the goal of $O[(v/c)^{11}]$ is achievable. The most difficult part of the computation, the radiation reaction, has been evaluated to $O[(v/c)^9]$ beyond Newton by the French/Indian/American consortium [28] and as of this writing, rumors have it that $O[(v/c)^{10}]$ is coming under control.

These high-accuracy waveforms are needed only for extracting information from the inspiral waves, after the waves have been discovered; they are not needed for the discovery itself. The discovery is best achieved using a different family of theoretical waveform templates, one that covers the space of potential waveforms in a manner that minimizes computation time instead of a manner that ties quantitatively into general relativity theory [18]. Such templates are in the early stage of development [35, 36, 37].

LIGO/VIRGO observations of compact binary inspiral have the potential to bring us far more information than just binary masses and spins:

– They can be used for high-precision tests of general relativity. In scalar-tensor theories (some of which are highly attractive alternatives to general relativity [38]), radiation reaction due to emission of scalar waves places a unique signature on those waves that LIGO/VIRGO would detect—a signature that can be searched for with high precision

[39].

– They can be used to measure the Hubble constant, deceleration parameter, and cosmological constant [16, 17, 40, 41]. The keys to such measurements are that (i) advanced interferometers in LIGO/VIRGO will be able to see NS/NS out to cosmological redshifts $z \sim 0.3$, and NS/BH out to $z \sim 2$. (ii) The direct observables that can be extracted from the observed waves include the source's luminosity distance $r_{\rm L}$ (measured to accuracy ~ 10 per cent in a large fraction of cases), and its direction on the sky (to accuracy ~ 1 square degree)—accuracies good enough that only one or a few electromagnetically-observed clusters of galaxies should fall within the 3-dimensional gravitational error boxes, thereby giving promise to joint gravitational/electromagnetic statistical studies. (iii) Another direct gravitational observable is $(1+z)M$ where z is redshift and M is any mass in the system (measured to the accuracies quoted above). Since the masses of NS's in binaries seem to cluster around $1.4M_\odot$, measurements of $(1+z)M$ can provide a handle on the redshift, even in the absence of electromagnetic aid.
– For a NS or small BH spiraling into a massive ~ 50 to $500M_\odot$ BH, the inspiral waves will carry a "map" of the spacetime geometry around the big hole—a map that can be used, e.g., to test the theorem that "a black hole has no hair" [42]; cf. Sec. 5.3 below.

3.1.4. *Coalescence Waveforms and their Information*

The waves from the binary's final coalescence can bring us new types of information.

BH/BH Coalescence: In the case of a BH/BH binary, the coalescence will excite large-amplitude, highly nonlinear vibrations of spacetime curvature near the coalescing black-hole horizons—a phenomenon of which we have very little theoretical understanding today. Especially fascinating will be the case of two spinning black holes whose spins are not aligned with each other or with the orbital angular momentum. Each of the three angular momentum vectors (two spins, one orbital) will drag space in its vicinity into a tornado-like swirling motion—the general relativistic "dragging of inertial frames," so the binary is rather like two tornados with orientations skewed to each other, embedded inside a third, larger tornado with a third orientation. The dynamical evolution of such a complex configuration of spacetime warpage (as revealed by its emitted waves) may well bring us surprising new insights into relativistic gravity. Moreover, if the sum of the BH masses is fairly large, ~ 40 to $200M_\odot$, then the waves should come off in a frequency range $f \sim 40$ to 200 Hz where the LIGO/VIRGO broadband interferometers have their best sensitivity and can best extract the information the waves carry.

To get full value out of such wave observations will require having theoretical computations with which to compare them [43]. There is no hope to perform such computations analytically; they can only be done as supercomputer simulations. The development of such simulations is a major effort within the world's relativity community.

NS/NS Coalescence: The final coalescence of NS/NS binaries should produce waves that are sensitive to the equation of state of nuclear matter, so such coalescences have the potential to teach us about the nuclear equation of state [18]. In essence, we will be studying nuclear physics via the collisions of atomic nuclei that have nucleon numbers $A \sim 10^{57}$—somewhat larger than physicists are normally accustomed to. The accelerator used to drive these nuclei up to the speed of light is the binary's self gravity, and the radiation by which the details of the collisions are probed is gravitational.

A number of research groups [44, 45, 46, 47, 13, 14, 48, 49] are engaged in numerical astrophysics simulations of NS/NS coalescence, with the goal not only to predict the emitted gravitational waveforms and their dependence on equation of state, but also (more immediately) to learn whether such coalescences might power the γ-ray bursts that have been a major astronomical puzzle since their discovery in the early 1970s. If advanced LIGO interferometers were now in operation, they could report definitively whether or not the γ-bursts are produced by NS/NS binaries; and if the answer were yes, then the combination of γ-burst data and gravitational-wave data could bring valuable information that neither could bring by itself. For example, we could determine when, to within a few msec, the γ-burst is emitted relative to the moment the NS's first begin to touch; and by comparing the γ and gravitational times of arrival, we might test whether gravitational waves propagate with the speed of light to a fractional precision of $\sim 0.01\text{sec}/3 \times 10^9\,\text{lyr} \sim 10^{-19}$.

Unfortunately, the final NS/NS coalescence will emit its gravitational waves in the kHz frequency band (800Hz $\lesssim f \lesssim$ 2500Hz) where photon shot noise will prevent them from being studied by the standard, "workhorse," broad-band interferometers of Fig. 3. However, a specially configured ("dual-recycled") interferometer invented by Brian Meers [50], which could have enhanced sensitivity in the kHz region at the price of reduced sensitivity elsewhere, may be able to measure the waves and extract their equation of state information, as might massive, spherical bar detectors [18, 51]. Such measurements will be very difficult and are likely only when the LIGO/VIRGO network has reached a mature stage.

NS/BH Coalescence: A NS spiraling into a BH of mass $M \gtrsim 10M_\odot$ should be swallowed more or less whole. However, if the BH is less massive than roughly $10M_\odot$, and especially if it is rapidly rotating, then the NS will tidally disrupt before being swallowed. Little is known about the disruption

and accompanying waveforms. To model them with any reliability will likely require full numerical relativity, since the circumferences of the BH and NS will be comparable and their physical separation at the moment of disruption will be of order their separation. As with NS/NS, the coalescence waves should carry equation of state information and will come out in the kHz band, where their detection will require advanced, specialty detectors.

Christodoulou Memory: As the coalescence waves depart from their source, their energy creates (via the nonlinearity of Einstein's field equations) a secondary wave called the "Christodoulou memory" [52, 53, 54]. Whereas the primary waves may have frequencies in the kHz band, the memory builds up on the timescale of the primary energy emission profile, which is likely to be of order 0.01 sec, corresponding to a memory frequency in the optimal band for the LIGO/VIRGO workhorse interferometers, $\sim$ 100Hz. Unfortunately, the memory is so weak that only very advanced interferometers have much chance of detecting and studying it—and then, perhaps only for BH/BH coalescences and not for NS/NS or NS/BH [55].

3.2. STELLAR CORE COLLAPSE AND SUPERNOVAE

Several features of the stellar core collapse, which triggers supernovae, can produce significant gravitational radiation in the high-frequency band. We shall consider these features in turn, the most weakly radiating first.

3.2.1. *Boiling of the Newborn Neutron Star*

Even if the collapse is spherical, so it cannot radiate any gravitational waves at all, it should produce a convectively unstable neutron star that "boils" vigorously (and nonspherically) for the first ~ 0.1 second of its life [56]. The boiling dredges up high-temperature nuclear matter ($T \sim 10^{12}$K) from the neutron star's central regions, bringing it to the surface (to the "neutrinosphere"), where it cools by neutrino emission before being swept back downward and reheated. Burrows estimates [57, 58] that the boiling should generate $n \sim 10$ cycles of gravitational waves with frequency $f \sim 100$Hz and amplitude $h \sim 3 \times 10^{-22}(30\text{kpc}/r)$ (where r is the distance to the source), corresponding to a characteristic amplitude $h_c \simeq h\sqrt{n} \sim 10^{-21}(30\text{kpc}/r)$; cf. Fig. 6. LIGO/VIRGO will be able to detect such waves only in the local group of galaxies, where the supernova rate is probably no larger than ~ 1 each 10 years. However, neutrino detectors have a similar range, and there could be a high scientific payoff from correlated observations of the gravitational waves emitted by the boiling's mass motions and neutrinos emitted from the boiling neutrino-sphere.

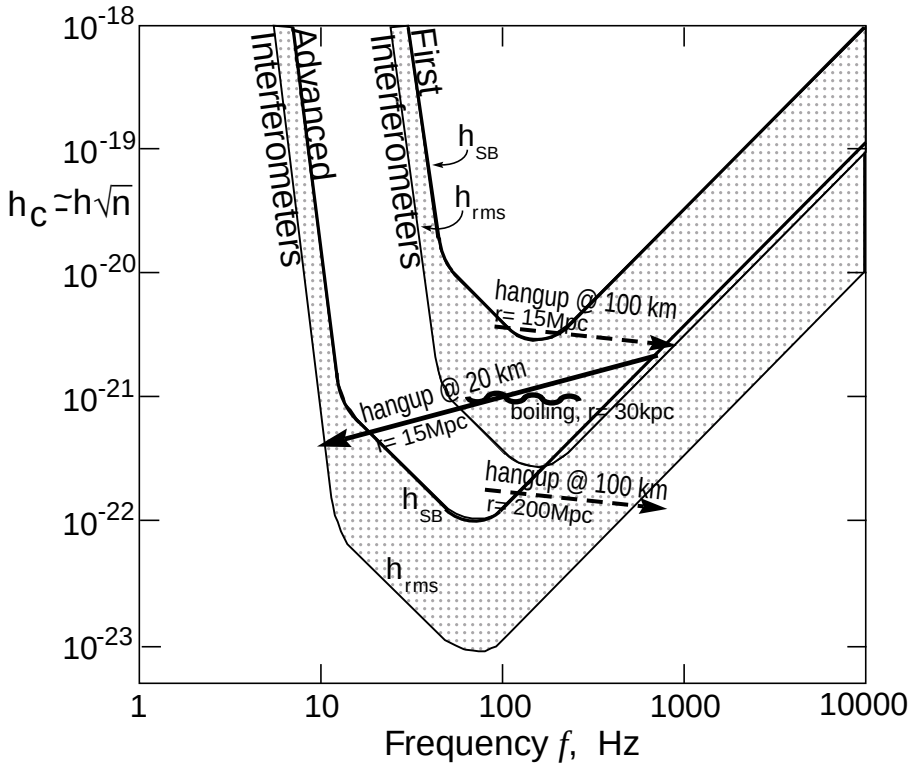

Figure 6. Characteristic amplitudes of the gravitational waves from various processes accompanying stellar core collapse and supernovae, compared with projected sensitivities of LIGO's interferometers.

3.2.2. *Axisymmetric Collapse, Bounce, and Oscillations*

Rotation will centrifugally flatten the collapsing core, enabling it to radiate as it implodes. If the core's angular momentum is small enough that centrifugal forces do not halt or strongly slow the collapse before it reaches nuclear densities, then the core's collapse, bounce, and subsequent oscillations are likely to be axially symmetric. Numerical simulations [59, 60] show that in this case the waves from collapse, bounce, and oscillation will be quite weak: the total energy radiated as gravitational waves is not likely to exceed $\sim 10^{-7}$ solar masses (about 1 part in a million of the collapse energy) and might often be much less than this; and correspondingly, the waves' characteristic amplitude will be $h_c \lesssim 3 \times 10^{-21}(30\text{kpc}/r)$. These collapse-and-bounce waves will come off at frequencies ~ 200 Hz to ~ 1000 Hz, and will precede the boiling waves by a fraction of a second. Like the boiling waves, they probably cannot be seen by LIGO/VIRGO beyond the local group of galaxies and thus will be a very rare occurrence.

3.2.3. *Rotation-Induced Bars and Break-Up*

If the core's rotation is large enough to strongly flatten the core before or as it reaches nuclear density, then a dynamical and/or secular instability is likely to break the core's axisymmetry. The core will be transformed into a bar-like configuration that spins end-over-end like an American football, and that might even break up into two or more massive pieces. In this case, the radiation from the spinning bar or orbiting pieces *could* be almost as strong as that from a coalescing neutron-star binary, and thus could be seen by the LIGO/VIRGO first interferometers out to the distance of the Virgo cluster (where the supernova rate is several per year) and by advanced interferometers out to several hundred Mpc (supernova rate $\sim 10^4$ per year); cf. Fig. 6. It is far from clear what fraction of collapsing cores will have enough angular momentum to break their axisymmetry, and what fraction of those will actually radiate at this high rate; but even if only $\sim 1/1000$ or $1/10^4$ do so, this could ultimately be a very interesting source for LIGO/VIRGO.

Several specific scenarios for such non-axisymmetry have been identified:

Centrifugal hangup at $\sim$ 100km radius: If the pre-collapse core is rapidly spinning (e.g., if it is a white dwarf that has been spun up by accretion from a companion), then the collapse may produce a highly flattened, centrifugally supported disk with most of its mass at radii $R \sim 100$km, which then (via instability) may transform itself into a bar or may bifurcate. The bar or bifurcated lumps will radiate gravitational waves at twice their rotation frequency, $f \sim 100$Hz — the optimal frequency for LIGO/VIRGO interferometers. To shrink on down to ~ 10km size, this configuration must shed most of its angular momentum. *If* a substantial fraction of the angular momentum goes into gravitational waves, then independently of the strength of the bar, the waves will be nearly as strong as those from a coalescing binary. The reason is this: The waves' amplitude h is proportional to the bar's ellipticity e, the number of cycles n of wave emission is proportional to $1/e^2$, and the characteristic amplitude $h_c = h\sqrt{n}$ is thus independent of the ellipticity and is about the same whether the configuration is a bar or is two lumps [17]. The resulting waves will thus have h_c roughly half as large, at $f \sim 100$Hz, as those from a NS/NS binary (half as large because each lump might be half as massive as a NS), and they will chirp upward in frequency in a manner similar to those from a binary.

It is rather likely, however, that most of the excess angular momentum does *not* go into gravitational waves, but instead goes largely into hydrodynamic waves as the bar or lumps, acting like a propeller, stir up the surrounding stellar mantle. In this case, the radiation will be correspondingly weaker.

Centrifugal hangup at R $\sim$ 20km: Lai and Shapiro [61] have ex-

plored the case of centrifugal hangup at radii not much lager than the final neutron star, say $R \sim 20$km. Using compressible ellipsoidal models, they have deduced that, after a brief period of dynamical bar-mode instability with wave emission at $f \sim 1000$Hz (explored by Houser, Centrella, and Smith [62]), the star switches to a secular instability in which the bar's angular velocity gradually slows while the material of which it is made retains its high rotation speed and circulates through the slowing bar. The slowing bar emits waves that sweep *downward* in frequency through the LIGO/VIRGO optimal band $f \sim 100$Hz, toward ~ 10Hz. The characteristic amplitude (Fig. 6) is only modestly smaller than for the upward-sweeping waves from hangup at $R \sim 100$km, and thus such waves should be detectable near the Virgo Cluster by the first LIGO/VIRGO interferometers, and at distances of a few 100Mpc by advanced interferometers.

Successive fragmentations of an accreting, newborn neutron star: Bonnell and Pringle [63] have focused on the evolution of the rapidly spinning, newborn neutron star as it quickly accretes more and more mass from the pre-supernova star's inner mantle. If the accreting material carries high angular momentum, it may trigger a renewed bar formation, lump formation, wave emission, and coalescence, followed by more accretion, bar and lump formation, wave emission, and coalescence. Bonnell and Pringle speculate that hydrodynamics, not wave emission, will drive this evolution, but that the total energy going into gravitational waves might be as large as $\sim 10^{-3} M_\odot$. This corresponds to $h_c \sim 10^{-21}(10\text{Mpc}/r)$.

3.3. SPINNING NEUTRON STARS; PULSARS

As the neutron star settles down into its final state, its crust begins to solidify (crystalize). The solid crust will assume nearly the oblate axisymmetric shape that centrifugal forces are trying to maintain, with poloidal ellipticity $\epsilon_p \propto$(angular velocity of rotation)^2. However, the principal axis of the star's moment of inertia tensor may deviate from its spin axis by some small "wobble angle" θ_w, and the star may deviate slightly from axisymmetry about its principal axis; i.e., it may have a slight ellipticity ϵ_e in its equatorial plane.

As this slightly imperfect crust spins, it will radiate gravitational waves [64]: ϵ_e radiates at twice the rotation frequency, $f = 2f_{\rm rot}$ with $h \propto \epsilon_e$, and the wobble angle couples to ϵ_p to produce waves at $f = f_{\rm rot} + f_{\rm prec}$ (the precessional sideband of the rotation frequency) with amplitude $h \propto \theta_w \epsilon_p$. For typical neutron-star masses and moments of inertia, the wave amplitudes are

$$h \sim 6 \times 10^{-25} \left(\frac{f_{\rm rot}}{500\text{Hz}}\right)^2 \left(\frac{1\text{kpc}}{r}\right) \left(\frac{\epsilon_e \text{ or } \theta_w \epsilon_p}{10^{-6}}\right) . \qquad (3)$$

The neutron star gradually spins down, due in part to gravitational-wave emission but perhaps more strongly due to electromagnetic torques associated with its spinning magnetic field and pulsar emission. This spin-down reduces the strength of centrifugal forces, and thereby causes the star's poloidal ellipticity ϵ_p to decrease, with an accompanying breakage and resolidification of its crust's crystal structure (a "starquake") [65]. In each starquake, θ_w, ϵ_e, and ϵ_p will all change suddenly, thereby changing the amplitudes of the star's two gravitational "spectral lines" $f = 2f_{\rm rot}$ and $f = f_{\rm rot} + f_{\rm prec}$. After each quake, there should be a healing period in which the star's fluid core and solid crust, now rotating at different speeds, gradually regain synchronism. By monitoring the amplitudes, frequencies, and phases of the two gravitational-wave spectral lines, and by comparing with timing of the electromagnetic pulsar emission, one might learn much about the physics of the neutron-star interior.

How large will the quantities ϵ_e and $\theta_w\epsilon_p$ be? Rough estimates of the crustal shear moduli and breaking strengths suggest an upper limit in the range $\epsilon_{\rm max} \sim 10^{-4}$ to 10^{-6}, and it might be that typical values are far below this. We are extremely ignorant, and correspondingly there is much to be learned from searches for gravitational waves from spinning neutron stars.

One can estimate the sensitivity of LIGO/VIRGO (or any other broad-band detector) to the periodic waves from such a source by multiplying the waves' amplitude h by the square root of the number of cycles over which one might integrate to find the signal, $n = f\hat{\tau}$ where $\hat{\tau}$ is the integration time. The resulting effective signal strength, $h\sqrt{n}$, is larger than h by

$$\sqrt{n} = \sqrt{f\hat{\tau}} = 10^5 \left(\frac{f}{1000{\rm Hz}}\right)^{1/2} \left(\frac{\hat{\tau}}{4{\rm months}}\right)^{1/2} . \qquad (4)$$

This $h\sqrt{n}$ should be compared (i) to the detector's rms broad-band noise level for sources in a random direction, $\sqrt{5}h_{\rm rms}$, to deduce a signal-to-noise ratio, or (ii) to $h_{\rm SB}$ to deduce a sensitivity for high-confidence detection when one does not know the waves' frequency in advance [2]. Such a comparison suggests that the first interferometers in LIGO/VIRGO might possibly see waves from nearby spinning neutron stars, but the odds of success are very unclear.

The deepest searches for these nearly periodic waves will be performed by narrow-band detectors, whose sensitivities are enhanced near some chosen frequency at the price of sensitivity loss elsewhere—e.g., "dual recycled" interferometers or resonant bars. With "advanced-detector technology," dual-recycled interferometers might be able to detect with confidence all spinning neutron stars that have [2]

$$(\epsilon_e \text{ or } \theta_w\epsilon_p) \gtrsim 3 \times 10^{-10} \left(\frac{500{\rm Hz}}{f_{\rm rot}}\right)^2 \left(\frac{r}{1000{\rm pc}}\right)^2 . \qquad (5)$$

There may well be a large number of such neutron stars in our galaxy; but it is also conceivable that there are none. We are extremely ignorant.

Some cause for optimism arises from several physical mechanisms that might generate radiating ellipticities large compared to 3×10^{-10}:

- It may be that, inside the superconducting cores of many neutron stars, there are trapped magnetic fields with mean strength $B_{\rm core} \sim 10^{13}$G or even 10^{15}G. Because such a field is actually concentrated in flux tubes with $B = B_{\rm crit} \sim 6 \times 10^{14}$G surrounded by field-free superconductor, its mean pressure is $p_B = B_{\rm core}B_{\rm crit}/8\pi$. This pressure could produce a radiating ellipticity $\epsilon_{\rm e} \sim \theta_w \epsilon_p \sim p_B/p \sim 10^{-8} B_{\rm core}/10^{13}$G (where p is the core's material pressure).
- Accretion onto a spinning neutron star can drive precession (keeping θ_w substantially nonzero), and thereby might produce measurably strong waves [66].
- If a neutron star is born rotating very rapidly, then it may experience a gravitational-radiation-reaction-driven instability. In this "CFS" (Chandrasekhar, [67] Friedman, Schutz [68]) instability, density waves propagate around the star in the opposite direction to its rotation, but are dragged forward by the rotation. These density waves produce gravitational waves that carry positive energy as seen by observers far from the star, but negative energy from the star's viewpoint; and because the star thinks it is losing negative energy, its density waves get amplified. This intriguing mechanism is similar to that by which spiral density waves are produced in galaxies. Although the CFS instability was once thought ubiquitous for spinning stars, we now know that neutron star viscosity will kill it, stabilizing the star and turning off the waves, when the star's temperature is above some limit $\sim 10^{10}$K [69] and below some limit $\sim 10^9$K [70]; and correspondingly, the instability should operate only during the first few years of a neutron star's life, when $10^9 \mathrm{K} \lesssim T \lesssim 10^{10}$K.

4. LISA: The Laser Interferometer Space Antenna

Turn, now, from the high-frequency band, 1—10^4 Hz, to the low-frequency band, 10^{-4}—1 Hz. At present, the most sensitive gravitational-wave searches at low frequencies are those carried out by researchers at NASA's Jet propulsion Laboratory, using microwave-frequency Doppler tracking of interplanetary spacecraft. These searches are done at rather low cost, piggyback on missions designed for other purposes. Although they have a definite possibility of success, the odds are against them. Their best past sensitivities to bursts, for example, have been $h_{\rm SB} \sim 10^{-14}$, and prospects are good for reaching $\sim 10^{-15}$—10^{-16} in the next 5 to 10 years. However, the

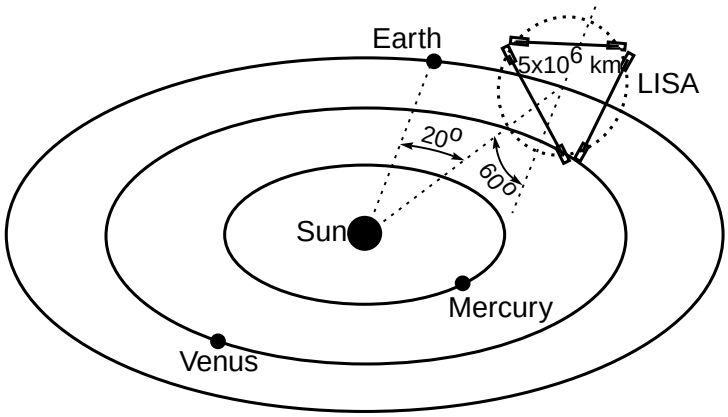

Figure 7. LISA's orbital configuration.

strongest low-frequency bursts arriving several times per year might be no larger than $\sim 10^{-18}$; and the domain of an assured plethora of signals is $h_{\rm SB} \sim 10^{-19}$—10^{-20}.

In the 2014 time frame, the European Space Agency (ESA) and/or NASA is likely to fly a *Laser Interferometer Space Antenna* (LISA) which will achieve $h_{\rm SB} \lesssim 10^{-20}$ over the frequency band $3 \times 10^{-4}{\rm Hz} \lesssim f \lesssim 3 \times 10^{-2}{\rm Hz}$.

4.1. MISSION STATUS

LISA is largely an outgrowth of 15 years of studies by Peter Bender and colleagues at the University of Colorado. Unfortunately, the prospects for NASA to fly such a mission have not looked good in the early 1990s. By contrast, prospects in Europe have looked much better, so a largely European consortium was put together in 1993 with Bender's participation but under the leadership of Karsten Danzmann (Hannover) and James Hough (Glasgow), to propose LISA to the European Space Agency. This proposal has met with considerable success; LISA might well achieve approval to fly as an ESA Cornerstone Mission around 2014 [71]. Members of the American gravitation community hope that NASA will join together with ESA in this endeavor, and that working jointly, ESA and NASA will be able to fly LISA considerably sooner than 2014.

4.2. MISSION CONFIGURATION

As presently conceived, LISA will consist of six compact, drag-free spacecraft (i.e. spacecraft that are shielded from buffeting by solar wind and radiation pressure, and that thus move very nearly on geodesics of space-

time). All six spacecraft would be launched simultaneously by a single Ariane rocket. They would be placed into the same heliocentric orbit as the Earth occupies, but would follow 20° behind the Earth; cf. Fig. 7. The spacecraft would fly in pairs, with each pair at the vertex of an equilateral triangle that is inclined at an angle of 60° to the Earth's orbital plane. The triangle's arm length would be 5 million km (10^6 times larger than LIGO's arms!). The six spacecraft would track each other optically, using one-Watt YAG laser beams. Because of diffraction losses over the 5×10^6km arm length, it is not feasible to reflect the beams back and forth between mirrors as is done with LIGO. Instead, each spacecraft will have its own laser; and the lasers will be phase locked to each other, thereby achieving the same kind of phase-coherent out-and-back light travel as LIGO achieves with mirrors. The six-laser, six-spacecraft configuration thereby functions as three, partially independent but partially redundant, gravitational-wave interferometers.

4.3. NOISE AND SENSITIVITY

Figure 8 depicts the expected noise and sensitivity of LISA in the same language as we have used for LIGO (Fig. 3). The curve at the bottom of the stippled region is $h_{\rm rms}$, the rms noise, in a bandwidth equal to frequency, for waves with optimum direction and polarization. The top of the stippled region is $h_{\rm SB} = 5\sqrt{5}h_{\rm rms}$, the sensitivity for high-confidence detection ($S/N = 5$) of a broad-band burst coming from a random direction, assuming Gaussian noise.

At frequencies $f \gtrsim 10^{-3}$Hz, LISA's noise is due to photon counting statistics (shot noise). The noise curve steepens at $f \sim 3 \times 10^{-2}$Hz because at larger f than that, the waves' period is shorter than the round-trip light travel time in one of LISA's arms. Below 10^{-3}Hz, the noise is due to buffeting-induced random motions of the spacecraft that are not being properly removed by the drag-compensation system. Notice that, in terms of dimensionless amplitude, LISA's sensitivity is roughly the same as that of LIGO's first interferometers (Fig. 3), but at 100,000 times lower frequency. Since the waves' energy flux scales as f^2h^2, this corresponds to 10^{10} better energy sensitivity than LIGO.

4.4. OBSERVATIONAL STRATEGY

LISA can detect and study, simultaneously, a wide variety of different sources scattered over all directions on the sky. The key to distinguishing the different sources is the different time evolution of their waveforms. The key to determining each source's direction, and confirming that it is real and not just noise, is the manner in which its waves' amplitude and

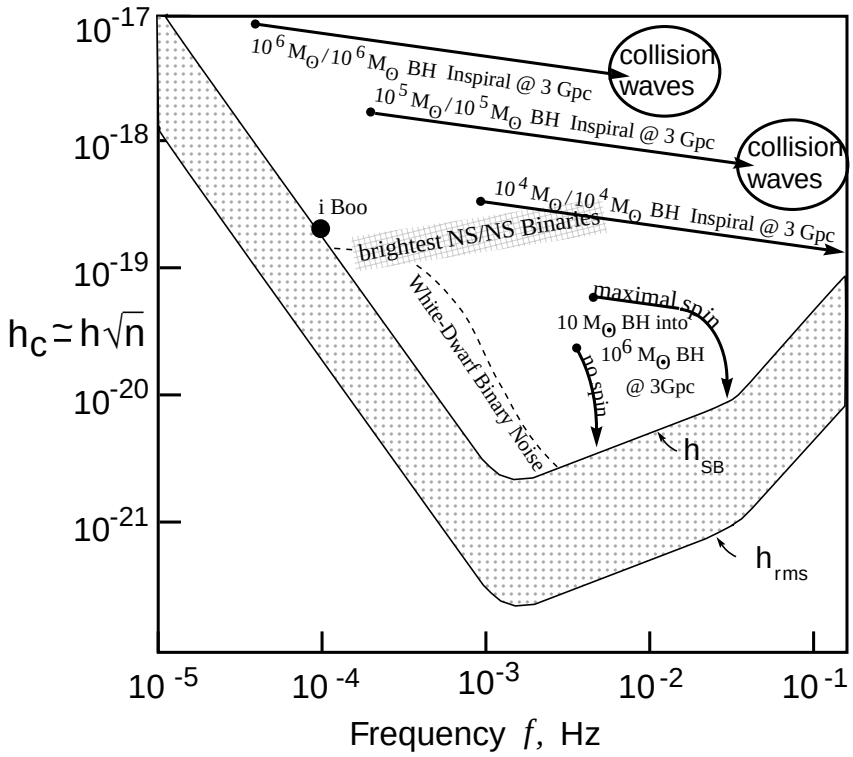

Figure 8. LISA's projected broad-band noise $h_{\rm rms}$ and sensitivity to bursts $h_{\rm SB}$, compared with the strengths of the waves from several low-frequency sources. [*Note:* When members of the LISA team plot curves analogous to this, they show the sensitivity curve (top of stippled region) in units of the amplitude of a periodic signal that can be detected with $S/N = 5$ in one year of integration; that sensitivity to periodic sources is related to the $h_{\rm SB}$ used here by $h_{\rm SP} = h_{\rm SB}/\sqrt{f \cdot 3 \times 10^7 \text{sec}}$.]

frequency are modulated by LISA's complicated orbital motion—a motion in which the interferometer triangle rotates around its center once per year, and the interferometer plane rotates around the normal to the Earth's orbit once per year. Most sources will be observed for a year or longer, thereby making full use of these modulations.

5. Low-Frequency Gravitational-Wave Sources

5.1. WAVES FROM BINARY STARS

LISA has a large class of guaranteed sources: short-period binary stars in our own galaxy. A specific example is the classic binary 44 i Boo (HD133640), a $1.35M_\odot$/ $0.68M_\odot$ system just 12 parsecs from Earth, whose wave frequency f and characteristic amplitude $h_c = h\sqrt{n}$ are depicted in Fig. 8.

(Here h is the waves' actual amplitude and $n = f\hat{\tau}$ is the number of wave cycles during $\hat{\tau}$ =1 year of signal integration.) Since 44 i Boo lies right on the $h_{\rm SB}$ curve, its signal to noise ratio in one year of integration should be $S/N = 5$.

To have an especially short period, a binary must be made of especially compact bodies—white dwarfs (WD), neutron stars (NS), and/or black holes (BH). WD/WD binaries are thought to be so numerous that they might produce a stochastic background of gravitational waves, at the level shown in Fig. 8, that will hide some other interesting waves from view [72]. Since WD/WD binaries are very dim optically, their actual numbers are not known for sure; Fig. 8 might be an overestimate.

Assuming a NS/NS coalescence rate of 1 each 10^5 years in our galaxy [6, 7], the shortest period NS/NS binary should have a remaining life of about 5×10^4 years, corresponding to a gravitational-wave frequency today of $f \simeq 5 \times 10^{-3}$Hz, an amplitude (at about 10kpc distance) $h \simeq 4 \times 10^{-22}$, and a characteristic amplitude (with one year of integration time) $h_c \simeq 2 \times 10^{-19}$. This is depicted in Fig. 8 at the right edge of the region marked "brightest NS/NS binaries". These brightest NS/NS binaries can be studied by LISA with the impressive signal to noise ratios $S/N \sim 50$ to 500.

5.2. WAVES FROM THE COALESCENCE OF MASSIVE BLACK HOLES IN DISTANT GALAXIES

LISA would be a powerful instrument for studying massive black holes in distant galaxies. Figure 8 shows, as examples, the waves from several massive black hole binaries at 3Gpc distance. The waves sweep upward in frequency (rightward in the diagram) as the holes spiral together. The black dots show the waves' frequency one year before the holes' final collision and coalescence, and the arrowed lines show the sweep of frequency and characteristic amplitude $h_c = h\sqrt{n}$ during that last year. For simplicity, the figure is restricted to binaries with equal-mass black holes: $10^4 M_\odot/10^4 M_\odot$, $10^5 M_\odot/10^5 M_\odot$, and $10^6 M_\odot/10^6 M_\odot$.

By extrapolation from these three examples, we see that LISA can study much of the last year of inspiral, and the waves from the final collision and coalescence, whenever the holes' masses are in the range $3 \times 10^4 M_\odot \lesssim M \lesssim 10^8 M_\odot$. Moreover, LISA can study the final coalescences with remarkable signal to noise ratios: $S/N \gtrsim 1000$. Since these are much larger S/N's than LIGO/VIRGO is likely to achieve, we can expect LISA to refine the experimental understanding of black-hole physics, and of highly nonlinear vibrations of warped spacetime, which LIGO/VIRGO initiates—*provided* the rate of massive black-hole coalescences is of order one per year in the Universe or higher. The rate might well be that high, but it also might be much lower.

By extrapolating Fig. 8 to lower BH/BH masses, we see that LISA can observe the last few years of inspiral, but not the final collisions, of binary black holes in the range $100M_\odot \lesssim M \lesssim 10^4 M_\odot$, out to cosmological distances.

Extrapolating the BH/BH curves to lower frequencies using the formula (time to final coalescence) $\propto f^{-8/3}$, we see that equal-mass BH/BH binaries enter LISA's frequency band roughly 1000 years before their final coalescences, more or less independently of their masses, for the range $100M_\odot \lesssim M \lesssim 10^6 M_\odot$. Thus, if the coalescence rate were to turn out to be one per year, LISA would see roughly 1000 additional massive binaries that are slowly spiraling inward, with inspiral rates df/dt readily measurable. From the inspiral rates, the amplitudes of the two polarizations, and the waves' harmonic content, LISA can determine each such binary's luminosity distance, redshifted chirp mass $(1+z)M_c$, orbital inclination, and eccentricity; and from the waves' modulation by LISA's orbital motion, LISA can learn the direction to the binary with an accuracy of some tens of arcminutes.

5.3. WAVES FROM COMPACT BODIES SPIRALING INTO MASSIVE BLACK HOLES IN DISTANT GALAXIES

When a compact body with mass μ spirals into a much more massive black hole with mass M, the body's orbital energy E at fixed frequency f (and correspondingly at fixed orbital radius a) scales as $E \propto \mu$, the gravitational-wave luminosity $\dot{E}$ scales as $\dot{E} \propto \mu^2$, and the time to final coalescence thus scales as $t \sim E/\dot{E} \propto 1/\mu$. This means that the smaller is μ/M, the more orbits are spent in the hole's strong-gravity region, $a \lesssim 10GM/c^2$, and thus the more detailed and accurate will be the map of the hole's spacetime geometry, which is encoded in the emitted waves.

For holes observed by LIGO/VIRGO, the most extreme mass ratio that we can hope for is $\mu/M \sim 1M_\odot/300M_\odot$, since for $M > 300M_\odot$ the inspiral waves are pushed to frequencies below the LIGO/VIRGO band. This limit on μ/M seriously constrains the accuracy with which LIGO/VIRGO can hope to map out the spacetime geometries of black holes and test the black-hole no-hair theorem (Sec. 3.1). By contrast, LISA can observe the final inspiral waves from objects of any mass $M \gtrsim 0.5M_\odot$ spiraling into holes of mass $3 \times 10^5 M_\odot \lesssim M \lesssim 3 \times 10^7 M_\odot$.

Figure 8 shows the example of a $10M_\odot$ black hole spiraling into a $10^6 M_\odot$ hole at 3Gpc distance. The inspiral orbit and waves are strongly influenced by the hole's spin. Two cases are shown [73]: an inspiraling circular orbit around a non-spinning hole, and a prograde, circular, equatorial orbit around a maximally spinning hole. In each case the dot at the upper left end of the arrowed curve is the frequency and characteristic ampli-

tude one year before the final coalescence. In the nonspinning case, the small hole spends its last year spiraling inward from $r \simeq 7.4GM/c^2$ (3.7 Schwarzschild radii) to its last stable circular orbit at $r = 6GM/c^2$ (3 Schwarzschild radii). In the maximal spin case, the last year is spent traveling from $r = 6GM/c^2$ (3 Schwarzschild radii) to the last stable orbit at $r = GM/c^2$ (half a Schwarzschild radius). The $\sim 10^5$ cycles of waves during this last year should carry, encoded in themselves, rather accurate values for the massive hole's lowest few multipole moments [74]. If the measured moments satisfy the "no-hair" theorem (i.e., if they are all determined uniquely by the measured mass and spin in the manner of the Kerr metric), then we can be sure the central body is a black hole. If they violate the no-hair theorem, then (assuming general relativity is correct), either the central body was not a black hole, or an accretion disk or other material was perturbing its orbit [75]. From the evolution of the waves one can hope to determine which is the case, and to explore the properties of the central body and its environment.

Models of galactic nuclei, where massive holes reside, suggest that inspiraling stars and small holes typically will be in rather eccentric orbits [76]. This is because they get injected into such orbits via gravitational deflections off other stars, and by the time gravitational radiation reaction becomes the dominant orbital driving force, there is not enough inspiral left to fully circularize their orbits. Such orbital eccentricity will complicate the waveforms and complicate the extraction of information from them. Efforts to understand the emitted waveforms are just now getting underway.

The event rates for inspiral into massive black holes are not at all well understood. However, since a significant fraction of all galactic nuclei are thought to contain massive holes, and since white dwarfs and neutron stars, as well as small black holes, can withstand tidal disruption as they plunge toward the massive hole's horizon, and since LISA can see inspiraling bodies as small as $\sim 0.5M_\odot$ out to 3Gpc distance, the event rate is likely to be interestingly large.

6. Conclusion

It is now 35 years since Joseph Weber initiated his pioneering development of gravitational-wave detectors [77] and 25 years since Forward and Weiss initiated work on interferometric detectors. Since then, hundreds of talented experimental physicists have struggled to improve the sensitivities of these instruments. At last, success is in sight. If the source estimates described in this lecture are approximately correct, then the planned interferometers should detect the first waves in 2001 or several years thereafter, thereby opening up this rich new window onto the universe. One payoff should

be deep new insights into compact astrophysical bodies and their roles in binary systems.

7. Acknowledgments

For insights into the rates of coalescence of compact binaries, I thank Sterl Phinney. My group's research on gravitational waves from compact bodies and the waves' relevance to LIGO/VIRGO and LISA is supported in part by NSF grants AST-9417371 and PHY-9424337 and by NASA grant NAGW-4268. This written version of my lecture has been adapted from a longer review article that I am writing for the Proceedings of the Snowmass '94 Summer Study on Particle and Nuclear Astrophysics and Cosmology in the Next Millenium.

References

1. A. Abramovici et. al. *Science*, 256:325, 1992.
2. K. S. Thorne. In S. W. Hawking and W. Israel, editors, *Three Hundred Years of Gravitation*, pages 330–458. Cambridge University Press, 1987.
3. C. Bradaschia et. al. *Nucl. Instrum. & Methods*, A289:518, 1990.
4. R. A. Hulse and J. H. Taylor. *Astrophys. J.*, 324:355, 1975.
5. J. H. Taylor. *Rev. Mod. Phys.*, 66:711, 1994.
6. E. S. Phinney. *Astrophys. J.*, 380:L17, 1991.
7. R. Narayan, T. Piran, and A. Shemi. *Astrophys. J.*, 379:L17, 1991.
8. M. Bailes. In J. van Paradijs, E. van den Heuvel, and E. Kuulkers, editors, *Proceedings of I. A. U. Symposium 165, Compact Stars in Binaries*. Kluwer Academic Publishers, 1995. in press.
9. A. V. Tutukov and L. R. Yungelson. *Mon. Not. Roy. Astron. Soc.*, 260:675, 1993.
10. H. Yamaoka, T. Shigeyama, and K. Nomoto. *Astron. Astrophys.*, 267:433, 1993.
11. E. P. J. van den Heuvel, 1994. preprint.
12. V. M. Lipunov, K. A. Postnov, and M. E. Prokhorov. *Astrophys. J.*, 423:L121, 1994. and related, unpublished work.
13. C. Kochanek. *Astrophys. J.*, 398:234, 1992.
14. L. Bildsten and C. Cutler. *Astrophys. J.*, 400:175, 1992.
15. G. Quinlan and S. L. Shapiro. *Astrophys. J.*, 321:199, 1987.
16. B. F. Schutz. *Nature*, 323:310, 1986.
17. B. F. Schutz. *Class. Quant. Grav.*, 6:1761, 1989.
18. C. Cutler, T. A. Apostolatos, L. Bildsten, L. S. Finn, E. E. Flanagan, D. Kennefick, D. M. Markovic, A. Ori, E. Poisson, G. J. Sussman, and K. S. Thorne. *Phys. Rev. Lett.*, 70:1984, 1993.
19. T. A. Apostolatos, C. Cutler, G. J. Sussman, and K. S. Thorne. *Phys. Rev. D*, 49:6274, 1994.
20. C. W. Lincoln and C. M. Will. *Phys. Rev. D*, 42:1123, 1990.
21. L. E. Kidder, C. M. Will, and A. G. Wiseman. *Phys. Rev. D*, 47:3281, 1993.
22. C. M. Will. In M. Sasaki, editor, *Relativistic Cosmology*, pages 83–98. Universal Academy Press, 1994.
23. L. E. Kidder. *Phys. Rev. D*, 1995. in press.
24. C. Cutler and E. E. Flanagan. *Phys. Rev. D*, 49:2658, 1994.
25. L. S. Finn and D. F. Chernoff. *Phys. Rev. D*, 47:2198, 1993.
26. E. Poisson and C. M. Will. *Phys. Rev. D*, 1995. submitted.
27. P. Jaranowski and A. Krolak. *Phys. Rev. D*, 49:1723, 1994.

28. L. Blanchet, T. Damour, B. R. Iyer, C. M. Will, and A. G. Wiseman. *Phys. Rev. Lett.*, 1995. submitted.
29. E. Poisson and M. Sasaki. *Phys. Rev. D*, 1995. in press.
30. M. Shibata, M. Sasaki, H. Tagoshi, and T. Tanaka. *Physical Review D*, 1995. in press.
31. H. Tagoshi and T. Nakamura. *Phys. Rev. D*, 49:4016, 1994.
32. H. Tagoshi and M. Sasaki. *Prog. Theor. Phys.*, 92:745, 1994.
33. C. Cutler and E. E. Flanagan. Phys. Rev. D. paper in preparation.
34. A. Ashtekar, ed. In N. Deruelle and T. Piran, editors, *Gravitational Radiation*, page 421, Amsterdam, 1983. North Holland.
35. A. Królak, K. D. Kokkotas, and G. Schäfer. *Proceedings of the 17th Texas Symposium on Relativistic Astrophysics, Ann. N. Y. Acad. Sci*, 1995. in press.
36. T. A. Apostolatos. *Phys. Rev. D*, 1995. in press.
37. B. S. Sathyaprakash. *Phys. Rev. D*, 50:R7111–R7115, 1994.
38. T. Damour and K. Nordtvedt. *Phys. Rev. D*, 48:3436, 1993.
39. C. M. Will. *Phys. Rev. D*, 50:6058, 1994.
40. D. Markovic. *Phys. Rev. D*, 48:4738, 1993.
41. D. F. Chernoff and L. S. Finn. *Astrophys. J. Lett.*, 411:L5, 1993.
42. F. Ryan, L. S. Finn, and K. S. Thorne. *Phys. Rev. Lett.*, 1995. in preparation.
43. E. E. Flanagan and S. A. Hughes. *Phys. Rev. D*, 1995. in preparation.
44. M. Shibata, T. Nakamura, and K. Oohara. *Prog. Theor. Phys.*, 88:1079, 1992.
45. M. Shibata, T. Nakamura, and K. Oohara. *Prog. Theor. Phys.*, 89:809, 1993.
46. F. A. Rasio and S. L. Shapiro. *Astrophys. J.*, 401:226, 1992.
47. T. Nakamura. In M. Sasaki, editor, *Relativistic Cosmology*, page 155. Universal Academy Press, 1994.
48. X. Zhuge, J. M. Centrella, and S. L. W. McMillan. *Phys. Rev. D*, 50:6247, 1994.
49. M. B. Davies, W. Benz, T. Piran, and F. K. Thielemann. *Astrophys. J.*, 431:742, 1994.
50. B. J. Meers. *Phys. Rev. D*, 38:2317, 1988.
51. D. Kennefick, D. Laurence, and K. S. Thorne. Phys. Rev. D. in preparation.
52. D. Christodoulou. *Phys. Rev. Lett.*, 67:1486, 1991.
53. K. S. Thorne. *Phys. Rev. D*, 45:520–524, 1992.
54. A. G. Wiseman and C. M. Will. *Phys. Rev. D*, 44:R2945, 1991.
55. D. Kennefick. *Phys. Rev. D*, 50:3587, 1994.
56. H. A. Bethe. *Rev. Mod. Phys*, 62:801, 1990.
57. A. Burrows, J. Hayes, and B. A. Fryxell. *Astrophys. J.*, 1995. in press.
58. A. Burrows, 1995. private communication.
59. L. S. Finn. *Ann. N. Y. Acad. Sci.*, 631:156, 1991.
60. R. Mönchmeyer, G. Schäfer, E. Müller, and R. E. Kates. *Astron. Astrophys.*, 256:417, 1991.
61. D. Lai and S. L. Shapiro. *Astrophys. J.*, 442:259, 1995.
62. J. L. Houser, J. M. Centrella, and S. C. Smith. *Phys. Rev. Lett.*, 72:1314, 1994.
63. I. A. Bonnell and J. E. Pringle. *Mon. Not. Roy. Astron. Soc.*, 273:L12, 1995.
64. M. Zimmermann and E. Szedenits. *Phys. Rev. D*, 20:351, 1979.
65. S. L. Shapiro and S. A. Teukolsky. Wiley: Interscience, 1983. Section 10.10 and references cited therein.
66. B. F. Schutz, 1995. private communication.
67. S. Chandrasekhar. *Phys. Rev. Lett.*, 24:611, 1970.
68. J. L. Friedman and B. F. Schutz. *Astrophys. J.*, 222:281, 1978.
69. L. Lindblom. *Astrophys. J.*, 438:265, 1995.
70. L. Lindblom and G. Mendell. *Astrophys. J.*, 444:804, 1995.
71. P. Bender, A. Brillet, I. Ciufolini, K. Danzmann, R. Hellings, J. Hough, A. Lobo, M. Sandford, B. Schutz, and P. Touboul. *LISA, Laser interferometer space antenna for gravitational wave measurements: ESA Assessment Study Report.* R. Reinhard, ESTEC, 1994.

72. D. Hils, P. Bender, and R. F. Webbink. *Astrophys. J.*, 360:75, 1990.
73. L. S. Finn and K. S. Thorne. *Phys. Rev. D*, 1995. in preparation.
74. F. Ryan. *Phys. Rev. D*, 1995. in preparation.
75. D. Molteni, G. Gerardi, and S. K. Chakrabarti. *Astrophys. J.*, 436:249, 1994.
76. D. Hils and P. Bender, 1995. preprint.
77. J. Weber. *Phys. Rev.*, 117:306, 1960.